



## Implementation of Carboxymethyl Cellulose/Acrylic acid/ Titanium Dioxide Nanocomposite Hydrogel in Remediation of Cd(II), Zn(II) and Pb(II) for Water Treatment Application



Ahmed A. Hendy<sup>1</sup>, Ehab E. Khozemy<sup>2</sup>, Ghada A. Mahmoud<sup>2\*</sup>, E. A. Saad<sup>3</sup>, Sherif H. Sorrow<sup>1</sup>

<sup>1</sup>Holding Company for Water and Wastewater (HCWW), Cairo, Egypt.

<sup>2</sup>National Center for Radiation Research and Technology, Atomic Energy Authority, P.O. Box 29, Nasr City, Cairo, Egypt.

<sup>3</sup>Faculty of Science, Ain Shams University, P.O. Box 68, Cairo, Egypt.

**I**N THIS study Acrylic acid/ Carboxymethylcellulose/Titanium dioxide (AAc/CMC-TiO<sub>2</sub>) hydrogel nanocomposite was synthesized by free-radical crosslinking copolymerization via gamma irradiation. It was characterized using FT-IR and swelling properties. The swelling percentage increases with increasing time until reaches a certain limiting value after 6h. The synthesized nanocomposite was used as an adsorbent for remediation of Cd(II), Zn(II) and Pb(II) from aqueous solutions by the static adsorption technique. It was found that the optimum pH for the adsorption is 5 and the sorption process is carried out at fast operating time, 30-40 min, for all investigated metal ions. It was also found that the metal ions sorption capacity decreases with increasing the dosage of AAc/CMC-TiO<sub>2</sub> from 5 to 150 mg. A progressive increase in the metal ions sorption capacity was obtained with increasing the initial metal ion concentration from 0.01 to 0.05 mol L<sup>-1</sup> and the saturation of the sorbent active sites was done at initial metal ions concentration at 0.1 mol L<sup>-1</sup>. No significant interference on the removal of Pb (II) in the presence of NaCl, Na-acetate, KCl, KNO<sub>3</sub> and NH<sub>4</sub>Cl ions while a slight decrease in removal of Cd (II) and Zn(II) was done. The pseudo-second order kinetic model and Freundlich adsorption model describe well the kinetic and isotherm, respectively, of the adsorption process of the investigated ions.

**Keywords:** Adsorption, Carboxymethyl cellulose, Gamma irradiation, Nanocomposite, Water treatment.

### Introduction

Hydrogels are three dimensional, porous, hydrophilic, physical and chemical crosslinking networks that swell thousands time of their dry weight in the vicinity of water [1]. These materials can respond to specific changes in their environment such as temperature, pH, magnetic field, and the electric field which determines their application in the fields of medicine, tissue engineering[2], wound dressing[3], biosensors[4], pharmaceutical[5], agriculture [6] and adsorption[7]. Hydrogels have found a special place in the field of wastewater treatments.

Factors affecting heavy metals adsorption by hydrogels are the structure, the type of pollutant, initial concentration of pollutants in the feed solution, treatment time, temperature and pH of pollutant solution [8]. Common functional groups that are used in synthesizing hydrogels include carboxylic acid, amide, amine, hydroxyl and sulfonic acid. Carboxymethylcellulose (CMC) is a biodegradable and biocompatible linear anionic polymer, the H atom of the hydroxyl cellulose group is replaced by carboxymethyl group -CH<sub>2</sub>-COOH [9]. Presence of monomers carrying -COOH groups play an important role

\*Corresponding author e-mail: ghadancrrt@yahoo.com; Phone: +2-01065495895; Fax: +2-022 2749298

Received 6/4/2019; Accepted 24/4/2019

DOI :10.21608/ejchem.2019.11622.1739

©2019 National Information and Documentation Center (NIDOC)

in the adsorption and swelling properties of hydrogels such as acrylic acid monomer. The presence -COOH groups have the ability to form a complex with metal cations [10]. In addition, the hydrogen bond between the polymer chains and water molecules are established because of the presence of -OH group. Due to the weak acidity of the carboxylic group, the behaviour of acrylic based hydrogels is sensitive to pH[11-13].

Nanosized metal oxides (NMOs) have been recognized by a number of physicochemical properties as high reactivity for separation, extraction and removal for organic and inorganic pollutants for the sake of water treatment[14]. NMOs, include nanosized aluminum, silicon, manganese, magnesium, ferric, cerium and titanium oxides. These nanomaterials have high surface area and excellent sorption capacity so they are used for removal of heavy metal ions[15]. Chitosan-coated-TiO<sub>2</sub> was applied to remove lead from aqueous solution[16]. Also, the nano-TiO<sub>2</sub>-glu-CMC nanocomposite was synthesized via glutaraldehyde crosslinking of Nano-TiO<sub>2</sub> with carboxymethyl cellulose (CMC). The nanocomposite was used for removal Cd(II), Hg(II) and Pb(II) ions from solutions[17].

Super absorbing poly(acrylic acid-co-acrylamide) hydrogels were synthesized by redox initiator and used for removal of Cu(II) ions from aqueous solutions[18]. Carboxylate grafted cellulose densified with TiO<sub>2</sub> was developed for extraction of uranium (VI) from aqueous solutions[19]. Chitosan-g-poly(acrylic acid) hydrogels were prepared from an aqueous dispersion polymerization method and used for removal of Ni(II)[20]. Environment-friendly carboxymethyl cellulose (CMC) hydrogel beads were successfully prepared using epichlorohydrin (ECH) as a crosslinking agent in the suspension of fluid wax And used for adsorption of Cu(II), Ni(II), and Pb(II)[21]. A series of functional copolymer hydrogels composed of carboxymethyl cellulose (CMC) and 2-acrylamido-2-methyl propane sulfonic acid (AMPS) were synthesized using gamma radiations-induced copolymerization and crosslinking to recover metal ions such as: Mn(II), Co(II), Cu(II), and Fe(III) from their solutions[22].

The present investigation aims to use AAc/CMC-TiO<sub>2</sub> hydrogel nanocomposite for remediation of heavy metal ions from aqueous

solutions. For this purpose, AAc/CMC-TiO<sub>2</sub> hydrogel nanocomposite was synthesized by free-radical crosslinking copolymerization of acrylic acid monomer with CMC polymer and TiO<sub>2</sub> via radiation-induced copolymerization using <sup>60</sup>Co gamma rays. The synthesized hydrogel nanocomposite was characterized using FT-IR and swelling properties. It was used as an adsorbent for remediation of Cd(II), Zn(II) and Pb(II) from aqueous solutions by the static adsorption technique in presence of different operational parameters such as pH, contact time, sorbent dosage, initial metal ion concentration and competing ions.

## Experimental

### *Material and chemicals*

Carboxy methyl cellulose sodium salt (CMC) was purchased from Qualikems, India. Acrylic acid was purchased from Alpha Chemika, India. Titanium dioxide Degussa P25 was supplied by Sigma-Aldrich Corp., Egypt. ammonium hydroxide was purchased from Scharlau, Spain. Cadmium sulfate octahydrate was purchased from Labo Chemie, India. Zinc Chloride was purchased from Scharlau, Spain. Hydrochloric acid was purchased from Sigma-Aldrich. Sodium acetate, ammonium chloride, lead acetate trihydrate and sulfuric acid were purchased from Sigma-Aldrich. Acidic solutions (pH 1.0, 2.0 and 3.0) were directly prepared from 1.0 mol L<sup>-1</sup>HCl acid, while buffer solutions (pH 4.0, 5.0, 6.0 and 7.0) were prepared by mixing the appropriate volume of 1.0 mol L<sup>-1</sup>HCl solution and 1.0 mol L<sup>-1</sup>NaAC. The total volumes of these solutions were made up to 500 mL and the final pH value was adjusted by a calibrated pH-meter. All chemicals are of analytical grades and were used without further purification.

### *Preparation of CMC based hydrogel nanocomposite*

AAc/CMC-TiO<sub>2</sub> hydrogel nanocomposite was prepared by free-radical crosslinking copolymerization of 20% acrylic acid monomer with 1% CMC polymer and 1%TiO<sub>2</sub> by radiation-induced copolymerization of mixture using <sup>60</sup>Co gamma rays at radiation dose 20 kGy using the facility of the National Center for Radiation Research and Technology, Cairo, Egypt. The obtained hydrogel nanocomposite was washed in excess water and soaked in distilled water for 24h at 60°C to remove the unreacted component, then air dried.

*Swelling studies*

The clean, dried, weighed sample was soaked in bi-distilled water at room temperature for different time intervals. The sample was taken and the excess water on the surface was removed by blotting quickly with a filter paper and reweighed. The swelling percent was calculated as follows:

$$\text{Swelling (\%)} = \frac{W_s - W_d}{W_d} \times 100 \quad (1)$$

Where  $W_d$  and  $W_s$  are the masses of dry and swelled sample, respectively.

*Fourier transform infrared spectrophotometer (FTIR)*

FTIR spectra were recorded on BRUKER Tensor 37 Fourier transform infrared spectrophotometer, in the range from 400–4000 $\text{cm}^{-1}$  using KBr pellets.

*Adsorption by batch equilibrium technique*

The batch equilibrium technique was used to study the influence of various experimental controlling factors in the processes of metal extraction by AAC/CMC-TiO<sub>2</sub> sorbent. These include the effect of pH, contact time, sorbent dosage, initial metal ion concentration and interfering ions. Each experiment was repeated three times according to the following procedures.

*The effect of pH on the sorption of selected metal ions*

50 ± 1.0 mg of AAC/CMC-TiO<sub>2</sub> sorbent was placed in a 15.0 mL volumetric tube and 1.0 mL of 0.1 mol L<sup>-1</sup> metal ions, Cd(II), Zn(II) and Pb(II), was added. After that 9.0 mL of the selected acidic or buffer solution was added to the reaction mixture and shaken at room temperature for 45.0 min. Then the mixture was filtered and the filtrate was titrated against 0.01 mol L<sup>-1</sup> EDTA by using the appropriate buffer solution and indicator. The sorption capacity value was calculated from Eq. (2).

$$q = \frac{(C_0 - C)}{m} \times V \quad (2)$$

where  $q$  (mmol g<sup>-1</sup>) represents the sorption metal ions capacity which is the amount of metal ion (mmol) adsorbed per gram of dry sorbent,  $C_0$  represents the initial concentration of metal ion,  $C$  (mol L<sup>-1</sup>) represents the residual concentration of metal ion,  $V$  (L) is the aqueous volume of the sorption reaction,  $m$  (g) is the mass of sorbent.

*The effect of contact time on the sorption of the selected metal ions*

50 ± 1.0 mg of AAC/CMC-TiO<sub>2</sub> sorbent was

placed in a 15.0 mL volumetric tube and 1.0 mL of 0.1 mol L<sup>-1</sup> metal ions, Cd(II), Zn(II) and Pb(II), was added. After that 9.0 mL of the selected acidic or buffer solution was added to the reaction mixture and shaken at room temperature for the selected time (1.0- 60.0 min). Then the mixture was filtered and the filtrate was titrated against 0.01 mol L<sup>-1</sup> EDTA by using the appropriate buffer solution and indicator. The sorption capacity value was calculated from Eq. (2).

*The effect of AAC/CMC-TiO<sub>2</sub> dose on the sorption of the selected metal ions*

The effect of dose of sorbent on the metal ions capacity was also studied by using various masses from 5.0mg to 150.0 mg of AAC/CMC-TiO<sub>2</sub> sorbent was added into a solution mixture of 1.0 mL of 0.1 mol L<sup>-1</sup> of Cd(II), Pb(II) or Zn(II) and 9 mL of optimum pH solution and shaken at room temperature for the optimum contact time. Then the mixture was filtered and the filtrate was titrated against 0.01 mol L<sup>-1</sup> EDTA by using the appropriate buffer solution and indicator. The sorption capacity value was calculated from Eq. (2).

*Effect of initial metal ion concentration on the sorption of the selected metal ions*

The effect of initial metal ion concentration was studied by the batch equilibrium technique using various concentrations of metal ions (0.01, 0.05, 0.1, 0.15 and 0.20 mol L<sup>-1</sup>) under the optimum conditions. The loaded sorbent-metal ion material was filtered and the collected filtrate was titrated with 0.01 mol L<sup>-1</sup> EDTA using the appropriate buffer solution and indicator. The sorption capacity value was calculated using Eq. (2).

*Effect of interfering ions on the sorption of the selected metal ions*

The effect of interfering ions on the sorption processes of Cd(II), Zn(II) and Pb(II) by AAC/CMC-TiO<sub>2</sub> sorbent was examined by the batch equilibrium technique. 1ml of 0.1 mol L<sup>-1</sup> each interfering species (NaCl, Na-acetate, KCl, KNO<sub>3</sub> and NH<sub>4</sub>Cl) was added to 1.0 mL of 0.1 mol L<sup>-1</sup> of the selected metal ion under the optimum conditions. The mixture was filtered and filtrate was titrated against 0.01 mol L<sup>-1</sup> of EDTA using the appropriate buffer and indicator and the removal percent was calculated in presence and absence of interfering ions.

## Result and Discussion

AAc/CMC-TiO<sub>2</sub> hydrogel nanocomposite is formed by the copolymerization and crosslinking of AAc and TiO<sub>2</sub> nanoparticles onto the CMC backbone using gamma radiation with a gelation percent of 95%. The hydrogel nanocomposite was swelled in distilled water at room temperature and the percentage of swelling was calculated at different time intervals as shown in Fig. 1. It can be seen that the swelling percentage of AAc/CMC-TiO<sub>2</sub> increases with increasing time until reaches a certain limiting value after 6h. The swelling rate increases up to the equilibrium which depends on the hydrophilicity of the polymer chains. When water comes to contact with the nanocomposite, water penetrates chains. The process is self-accelerating and the swollen matrix is formed.

The FT-IR spectra of CMC and AAc/CMC-TiO<sub>2</sub> hydrogel nanocomposite in the frequency range of 4000-400cm<sup>-1</sup> are shown in Fig. 2. The FTIR spectrum of CMC (Fig. 1a) is characterized by the presence of a characteristic absorption peak at 3411 cm<sup>-1</sup> related to OH groups. The presence of two strong peaks at 1618 cm<sup>-1</sup> and 1426cm<sup>-1</sup> correspond to the asymmetrical and symmetrical stretching vibration of -COO- groups, respectively [23]. CMC has also peaks at 1148 cm<sup>-1</sup>, 1023 cm<sup>-1</sup> and 2914cm<sup>-1</sup> are attributed to the anti-symmetric bridge C-O-C stretching vibration, C-O stretching vibration and C-H stretching vibration, respectively [24]. On the other hand, the FTIR spectrum of AAc/CMC-TiO<sub>2</sub> hydrogel nanocomposite (Fig. 1b) exhibits similar absorption peaks of CMC with

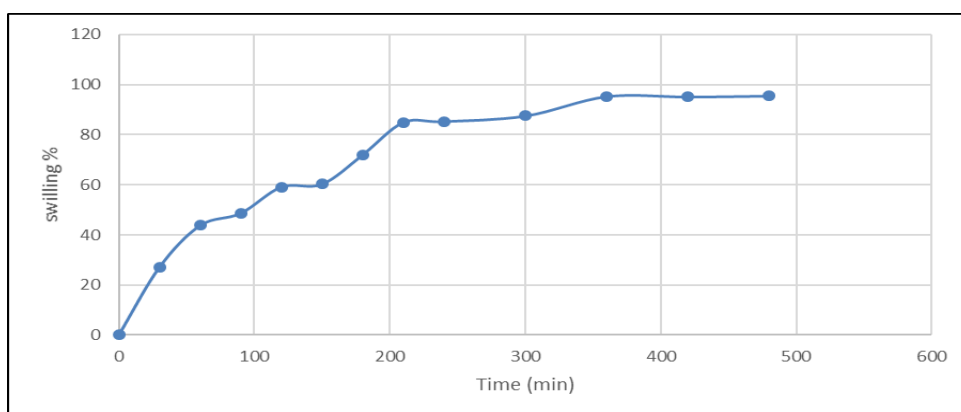


Fig. 1. Effect time on the swelling (%) AAc/CMC-TiO<sub>2</sub> hydrogel nanocomposite.

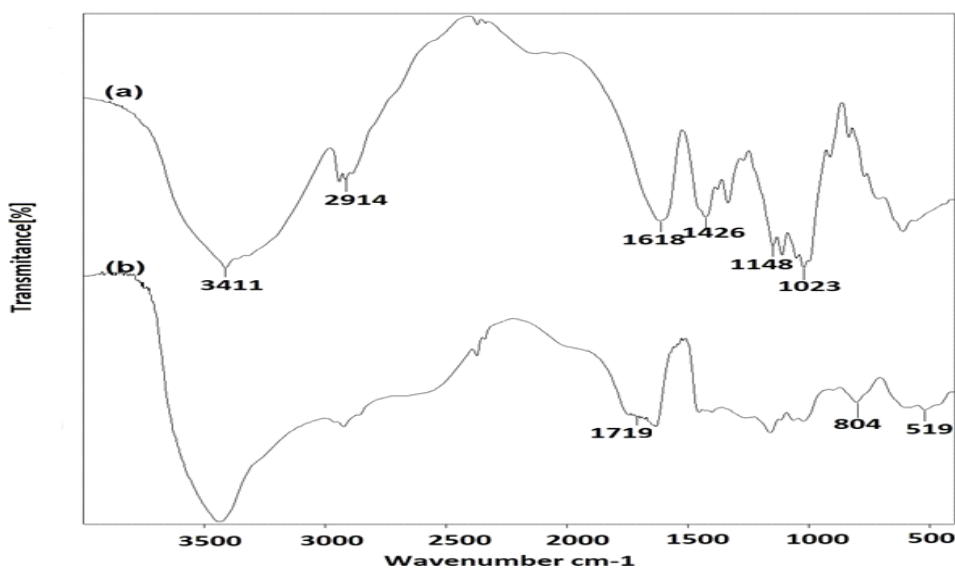


Fig. 2. FTIR spectra of CMC (a) and AAc/CMC-TiO<sub>2</sub> hydrogel nanocomposite (b).

some distinguishable differences as there are some peaks disappeared, others their intensity decreased and several new peaks appeared. The new peak appears at  $1719\text{ cm}^{-1}$  corresponds to the C=O groups of carboxylic acid moieties of AAc and two peaks at  $804\text{ cm}^{-1}$  and  $519\text{ cm}^{-1}$  attributed to Ti–O–Ti vibrations of  $\text{TiO}_2$  nanoparticles [17, 25, 26].

#### Adsorption properties

##### Effect of pH

The effect of pH on the adsorption is known to play a major important factor in such process because of the adsorption of most metal ions strongly affected by the surface loaded functional groups. The effect of pH on the adsorption of Cd(II), Zn(II) and Pb(II) by AAc/CMC- $\text{TiO}_2$  sorbent was investigated and are represented in Fig. 3. It was found that the increase of pH value of the metal ions solution, the sorption capacity value also increases for all investigated ions up to pH 5 above this value a decrease in adsorption was observed. In case of Cd(II),

the lowest detected sorption capacity value is identified as  $0.0488\text{ mmol g}^{-1}$  at pH 1.0 and the highest detected value is obtained at pH 5.0 as  $1.1183\text{ mmol g}^{-1}$ . The same behaviour were also recognized for Zn(II) and Pb(II) ions where the identified highest sorption capacity values are found at pH 5.0 as  $0.9512$  and  $1.6628\text{ mmol g}^{-1}$ , respectively, while the lowest detected sorption capacity values were found at pH 1.0 as  $0.1087$  and  $0.2520\text{ mmol g}^{-1}$ , respectively. This behaviour may be interpreted on the fact that in high acidic solutions, such as pH 1.0 and 3.0, the number of protons from aqueous solution is higher than the existing metal ions and thus most hydroxyl and carboxylic functional groups on the surface of AAc/CMC- $\text{TiO}_2$  sorbent are protonated. So that, the metal ions cannot interact with AAc/CMC- $\text{TiO}_2$  functional groups [17]. As the pH value of solution increases, the dissociation degree of functional groups also increases and the metal ions able to directly interact with the available functional groups [27]. However, at pH values

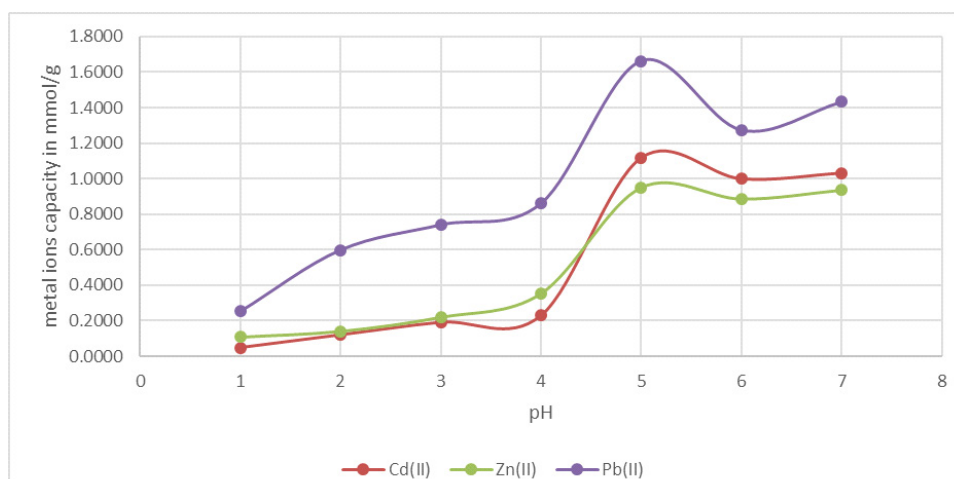


Fig. 3. Effect of pH on the metal ions capacity of Cd(II), Zn(II), and Pb(II) by AAc/CMC- $\text{TiO}_2$  hydrogel nanocomposite

higher than 5, the low sorption capacity values are obtained which are attributed to on one hand the precipitation of ions as hydroxides. On the other hand the interference caused by interaction between active sites and other interfering ions, which occupy active binding sites leading to inhibition of sorption process of the studied metals [17].

##### Effect of contact time

The effect of contact time on the metal ions sorption by AAc/CMC- $\text{TiO}_2$  was also studied at different time intervals (Fig. 4). It is concluded from this study that there is a gradual increase in

the sorption capacity values with the increase in the reaction contact time for all examined metal ions, Cd(II), Zn(II) and Pb(II) till reach to the saturation condition by adsorption on the surface of AAc/CMC- $\text{TiO}_2$  sorbent after 60.0 min. The sorption process of Cd(II), Zn(II) and Pb(II) by AAc/CMC- $\text{TiO}_2$  were found to proceed via two successive steps. The first step includes a rapid increase in the sorption capacities of Pb(II) at 1-40min and 1-30min for Cd(II) and Zn(II) onto AAc/CMC- $\text{TiO}_2$  sorbent due to the abundant availability of active sites on sorbent surface with gradual occupancy of these sites [28]. The

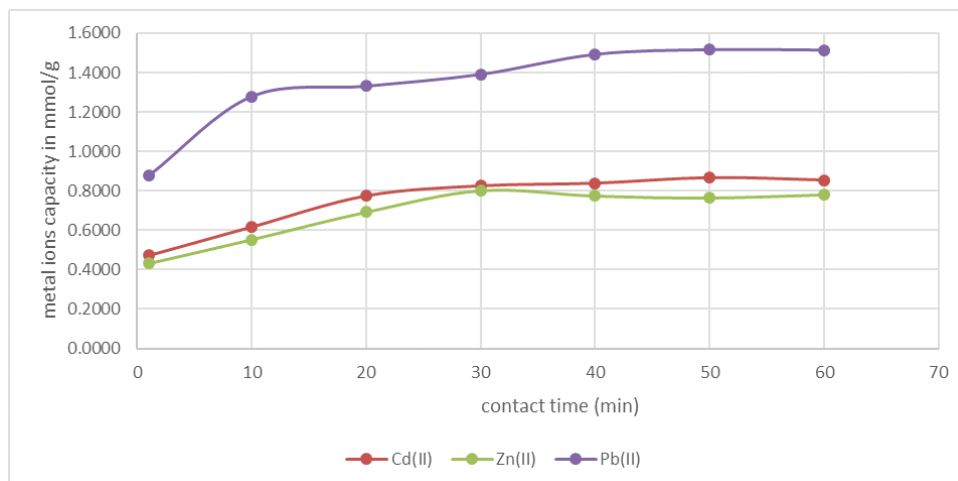


**Fig. 4.** Effect of contact time on the metal ions capacity of Cd(II), Zn(II), and Pb(II) by AAC/CMC-TiO<sub>2</sub> hydrogel nanocomposite.

second step, at which the equilibrium is reached, is mainly based on the complete saturation of the AAC/CMC-TiO<sub>2</sub> sorbent surface. It is clear from the study that sorption process of Cd(II), Zn(II) and Pb(II) is carried out at fast operating time 30-40 minutes. The identified optimum sorption capacity values were found as 0.8244, 0.8026 and 1.4932 mmol g<sup>-1</sup> for Cd(II), Zn(II) and Pb(II), respectively.

#### *Effect of sorbent dose*

The AAC/CMC-TiO<sub>2</sub> sorbent dosage was studied via optimum pH and contact time conditions for Cd(II), Zn(II) and Pb(II) with different masses of AAC/CMC-TiO<sub>2</sub> sorbent to evaluate its influence on the metal adsorption capacity values. Figure 5 illustrates the effect of AAC/CMC-TiO<sub>2</sub> dosage on the adsorption

processes. It is concluded from the results that the metal ions sorption capacity values decrease with increasing the mass of AAC/CMC-TiO<sub>2</sub> from 5 to 150 mg. The obtained highest metal capacities for Cd(II), Zn(II) and Pb(II) at 5mg AAC/CMC-TiO<sub>2</sub> sorbent were exhibited to be 3.2719, 2.5946 and 3.7300 mmol g<sup>-1</sup>, while the lowest metal capacities for Cd(II), Zn(II) and Pb(II) at 150 mg AAC/CMC-TiO<sub>2</sub> sorbent were exhibited to be 0.3769, 0.3580 and 0.5104 mmol g<sup>-1</sup>, respectively. This behaviour in low sorbent dosage was mainly attributed to the greater availability of metal ions compared to the active surface functional groups on the AAC/CMC-TiO<sub>2</sub> sorbent. On the other hand, the low metal ions adsorption capacity values at high mass were mainly due to the low number of available metal ions in aqueous solution compared with

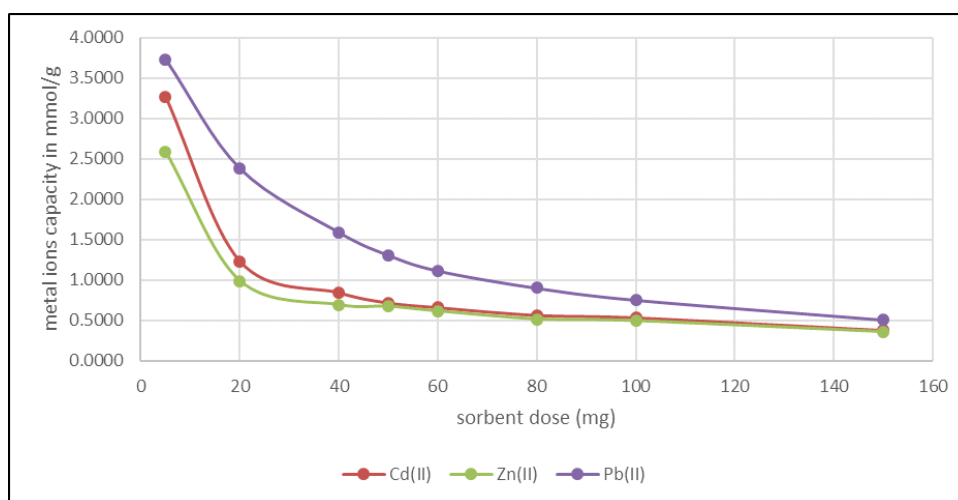


**Fig. 5.** Effect of sorbent dose on the metal ions capacity of Cd(II), Zn(II), and Pb(II) by AAC/CMC-TiO<sub>2</sub> hydrogel nanocomposite.

the availability of the functional groups on the adsorbent [29].

#### Effect of metal ion concentration

The effect of initial Cd(II), Zn(II) and Pb(II) concentrations on the adsorption process were investigated as shown in Fig. 6. The sorption capacity values of Cd(II), Zn(II) and Pb(II) were found to progressively increase upon increasing the initial metal ion concentration from 0.01 to 0.05 mol L<sup>-1</sup> due to the presence of high number of metal ions and accessible adsorption sites in contact solution followed by an insignificant increase in the sorption capacities from 0.05 to 0.1 mol L<sup>-1</sup> which may be due to saturation of the sorbent active sites

at initial metal ions concentration at 0.1 mol L<sup>-1</sup>. The maximum metal ions capacity values were found to be 1.3578, 1.3102 and 1.8569 mmol g<sup>-1</sup> Cd(II), Zn(II) and Pb(II), respectively, in presence of 0.10 mol L<sup>-1</sup> of initial metal ions concentration. At higher concentrations there is a high available number of ions compared to the limited number of surface functional groups on the sorbent [27, 30].

#### Effect of interfering ions

The removal percent of Cd (II), Zn (II) and Pb (II) by AAC/CMC-TiO<sub>2</sub> sorbent were investigated in presence of other interfering ions, such as NaCl, Na-acetate, KCl, KNO<sub>3</sub> and NH<sub>4</sub>Cl by using equimolar concentration of each metal ion. The results of this study are presented in Fig. 7 which

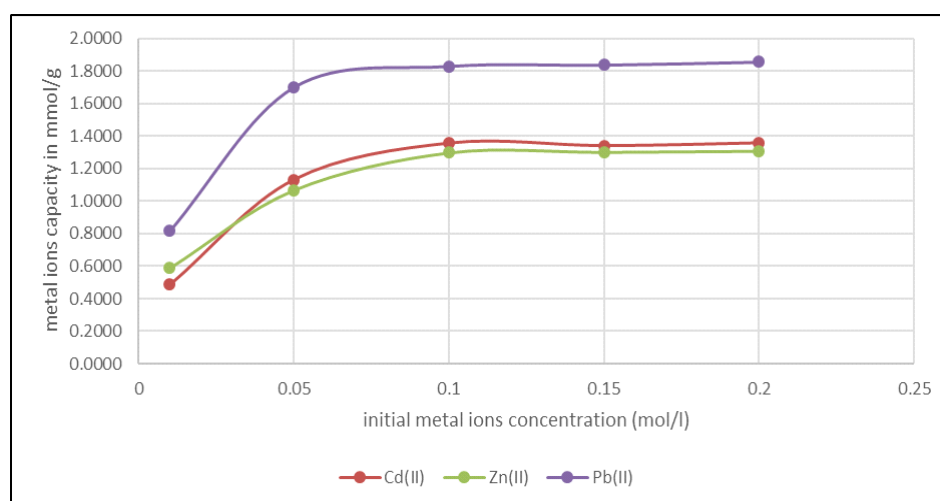


Fig. 6. Effect of initial metal ions concentration on the metal ions capacity of Cd(II), Zn(II), and Pb(II) by AAC/CMC-TiO<sub>2</sub> hydrogel nanocomposite.

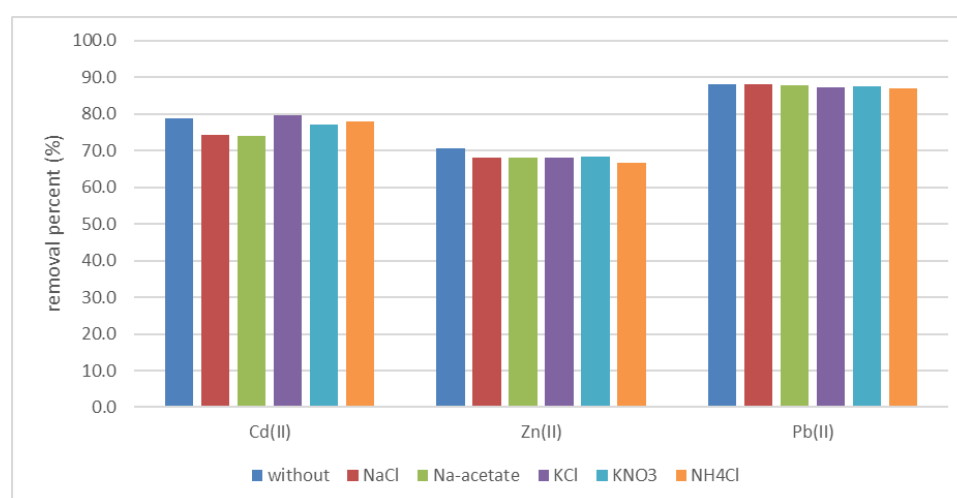


Fig. 7. Effect of the presence of other interfering ions on the removal percent of Cd(II), Zn(II), and Pb(II) by AAC/CMC-TiO<sub>2</sub> hydrogel nanocomposite.

indicate a good evaluation of removal percent in presence and absence of interfering ions. The presence of NaCl, Na-acetate, KCl,  $\text{KNO}_3$  and  $\text{NH}_4\text{Cl}$  ions were found to show non-significant interference on the removal of Pb (II) compared to removal in absence of interfering ions, while the presence of interfering ions slightly decrease the removal of Cd (II) and Zn(II).

#### Kinetic studies

The predicting rate at which the sorption takes

place for a given system is probably the most important factor in adsorption system design [31, 32]. Several kinetic models including: pseudo-first order, pseudo-second order, and intraparticle diffusion are used to examine the experimental data such as the examination of the controlling mechanisms of the adsorption process [33, 34]. The Pseudo-first order equation is generally expressed as follows [35, 36]

$$\log(q_e - q_t) = \log q_e - \frac{K_1}{2.303} t \quad (3)$$

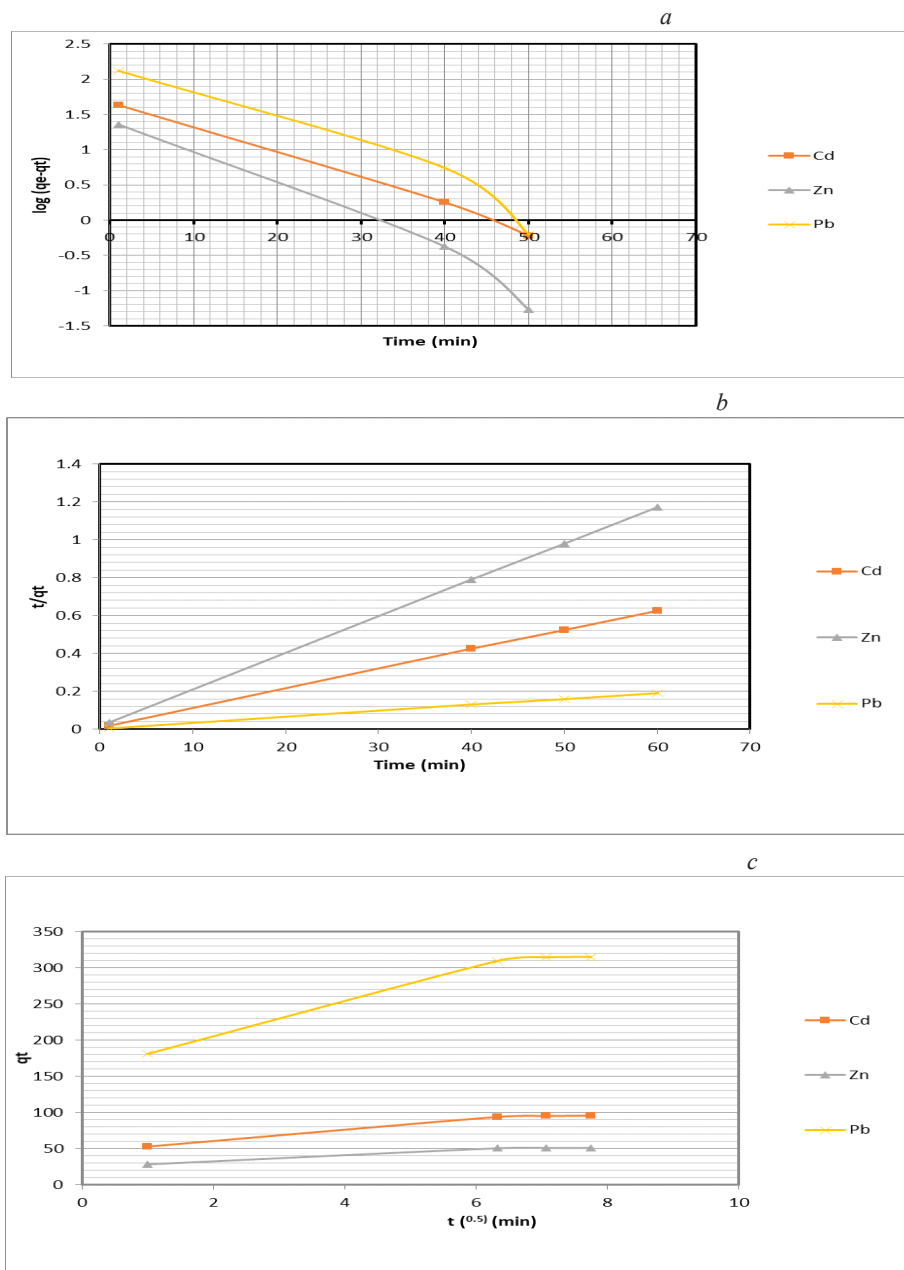


Fig. 8. Pseudo first order (a), Pseudo second order (b) and the intraparticle diffusion (c) kinetic plots for adsorption of Cd(II), Zn(II), and Pb(II) by AAC/CMC-TiO<sub>2</sub> hydrogel nanocomposite.

The straight-line plot of  $\log(q_e - q_t)$  versus  $t$  for the adsorption of Cd(II), Zn(II) and Pb(II) metal ions onto the nanosorbent has been tested to obtain the rate parameters as shown in Fig. 8 (a) and Table 1.

Data were applied to the pseudo-second order kinetic rate equation which is expressed as follows[34, 37]:

$$\frac{t}{q_t} = \frac{1}{k_2 q_e^2} + \frac{t}{q_e} \quad (4)$$

where,  $k_2$  is the equilibrium rate constant of pseudo-second order kinetic model (g/mg min). To understand the applicability of the model, linear plots of  $t/q_t$  versus  $t$  onto the studied nanosorbent were drawn as shown in Fig. 8 (b)  $k_2$ ,  $q_e$  and  $R^2$  were calculated from these plots and given in Table 1. The data in Table 1 show that the applicability of the pseudo-first order kinetic model and pseudo-second order kinetic model in describing the adsorption process of Cd(II), Zn(II) and Pb(II) metal ions onto the studied nanosorbent. However, the calculated correlation coefficients ( $R^2 > 0.999$ ) for pseudo-second order kinetic model is higher than pseudo-second order kinetic model. This reflects the applicability of this model in describing the adsorption process of Cd(II), Zn(II) and Pb(II) metal ions onto nanosorbent. This indicates that the initial metal ion concentration has an important role in the adsorption capacity of the studied nanosorbent.

The possibility of intraparticle diffusion resistance affecting the adsorption was explored by using the intraparticle diffusion model as follows[38]:

$$q_t = K_i t^{1/2} + C \quad (5)$$

where,  $K_i$  is the intraparticle diffusion rate constant. Plotting the adsorption capacity ( $q_t$ ) versus square root of adsorption time in minutes

( $t^{1/2}$ ) gave characteristic curves with three periods, as shown in Fig. 8(c). These periods are attributed to the adsorption stages of the exterior surface, interior surface, and equilibrium, respectively. The intraparticle diffusion model commonly divides the adsorption process into three stages[38]: the rapid surface adsorption stage, the gradual inward diffusion stage and the final equilibrium stage. In the first stage, adsorption takes place on exterior surface of adsorbent until the exterior surface is saturated by metal ions. The second stage takes place by entering the adsorbed metal ions into pores of adsorbents within the particle. When the metal ions diffused into adsorbent pores, the diffusion resistance increased due to crowding, and consequently the diffusion rate decrease. The third stage is the equilibrium between the metal ions in the solution and the adsorbed ions. This stage is very slow due to the decrease of metal ions concentration in the solution.

#### Adsorption isotherm studies

Several adsorption isotherms can be used to correlate the adsorption equilibria in heavy metals adsorption on several adsorbents. The well-known isotherms are: Langmuir and Freundlich models [39]. Langmuir isotherm assumes two main points in the adsorption process. First, the adsorption happens at specific homogeneous adsorption sites in the adsorbent. Second, the monolayer adsorption and maximum adsorption occurs when adsorbed molecules form a saturated layer on the surface of adsorbent. All adsorption sites involved are energetically identical and the intermolecular force decreases as the distance from the adsorption surface increases [40]. The Langmuir adsorption model can be represented by the following linearized form [40]:

$$\frac{c_e}{q_e} = \frac{1}{q_{max} k_l} + \frac{c_e}{q_{max}} \quad (6)$$

Where  $C_e$  is the equilibrium concentration (mg/L),  $q_e$  is the adsorbed metal ion (mg/g),  $q_{max}$  is  $q_e$  for a

**TABLE 1. Pseudo first order, Pseudo second order and the intraparticle diffusion kinetic parameters for adsorption of Cd(II), Zn(II), and Pb(II) by AAc/CMC-TiO<sub>2</sub> hydrogel nanocomposite.**

Metal ions	$q_{e, exp}$	1st order			2nd order			intra particle diffusion		
		$q_{e, cal}$	$K_1$	$R^2$	$q_{e, cal}$	$K_2$	$R^2$	$K(K_i)$	$I(C)$	$R^2$
Cd(II)	95.96	47.98	0.0854	0.9971	97.09	0.0109	0.9999	6.76	47.23	0.9762
Zn(II)	51.11	28.57	0.1177	0.9786	51.81	0.0227	1.0000	3.65	25.04	0.9698
Pb(II)	314.91	168.66	0.1018	0.9518	322.58	0.0036	0.9999	21.10	163.19	0.9760

complete monolayer (mg/g),  $K_1$  is constant related to the affinity of binding sites and is a measure of the energy of adsorption ( $L\ mg^{-1}$ ).

The Freundlich isotherm is an empirical equation assuming that the adsorption process takes place on heterogeneous surfaces and adsorption capacity is related to the concentration of adsorbed metal ions at equilibrium. Freundlich isotherm model is represented by the following

$$\ln q_e = \frac{1}{n} \ln C_e + \ln k_f \quad (7)$$

where  $k_f$  and  $n$  are constants related to the adsorption capacity and intensity, respectively.

In this study, Langmuir and Freundlich models were used to determine the adsorption equilibrium between the nano-sorbent and Cd(II), Zn(II) and Pb(II) metal ions as shown in Fig. 9. The isotherm constants for the two models were obtained by linear regression method and were listed in Table 2. In case of the two applied models, in Freundlich adsorption model, high correlation of the experimental and model data was obtained where the values of  $R^2$  were 0.9842, 0.9981 and 0.9906 for Cd(II), Zn(II) and Pb(II) metal ions, respectively. This means that Freundlich equilibrium isotherm well describes the metal adsorption process by the studied nanosorbent. Freundlich model provides two parameters:  $k_f$  which is related to the adsorption capacity and adsorption intensity of the different metal ions on nanosorbent, and  $n$  represents the strength of metal ions adsorption on the nanosorbent.

### Conclusion

Acrylic acid/ Carboxymethylcellulose/ Titanium dioxide (AAc/CMC-TiO<sub>2</sub>) hydrogel

nanocomposite was synthesized by free-radical crosslinking copolymerization via gamma radiation technique. The function group was confirmed by FT-IR analysis. The swelling properties was investigated and it was found that the swelling percentage increases with increasing time until reaches a certain limiting value after 6h. The synthesized nanocomposite was used as an adsorbent for remediation of Cd(II), Zn(II) and Pb(II) from aqueous solutions by the static adsorption technique. It was found that the sorption capacity increases with increasing pH for all investigated ions up to pH 5 above this value a decrease in adsorption was observed the precipitation of ions as hydroxides and the interaction between active sites and other interfering ions. The sorption process is carried out at fast operating time where the swelling equilibrium is obtained after 30 min for Cd(II) and Zn(II) and 40 min for Pb(II) ions. A progressive increase in the metal ions sorption capacity was obtained with increasing the initial metal ion concentration from 0.01 to 0.05 mol L<sup>-1</sup> and the saturation of the sorbent active sites was done at initial metal ions concentration at 0.1 mol L<sup>-1</sup>. The metal ions sorption capacity decreases with increasing the dosage of AAc/CMC-TiO<sub>2</sub> from 5 to 150 mg. No significant interference on the removal of Pb (II) in the presence of NaCl, Na-acetate, KCl, KNO<sub>3</sub> and NH<sub>4</sub>Cl ions while a slight decrease in removal of Cd (II) and Zn(II) was done. The Freundlich equilibrium isotherm describes well the metal ions adsorption process. The kinetic of adsorption follows the pseudo-second order kinetic model higher than the pseudo-first order kinetic model.

TABLE 2. Langmuir and Freundlich isotherm constants for adsorption of Cd(II), Zn(II), and Pb(II) by AAc/CMC-TiO<sub>2</sub> hydrogel nanocomposite.

Metal ions	Langmuir model			Freundlich model		
	R <sup>2</sup>	K <sub>1</sub>	q <sub>max</sub>	R <sup>2</sup>	n	k <sub>f</sub>
Cd(II)	0.0134	189.568	1666	0.9842	0.5577	0.00063
Zn(II)	0.0004	471.698	5000	0.9981	0.54283	0.00062
Pb(II)	0.8909	2558.461	5000	0.9906	0.73508	0.03346

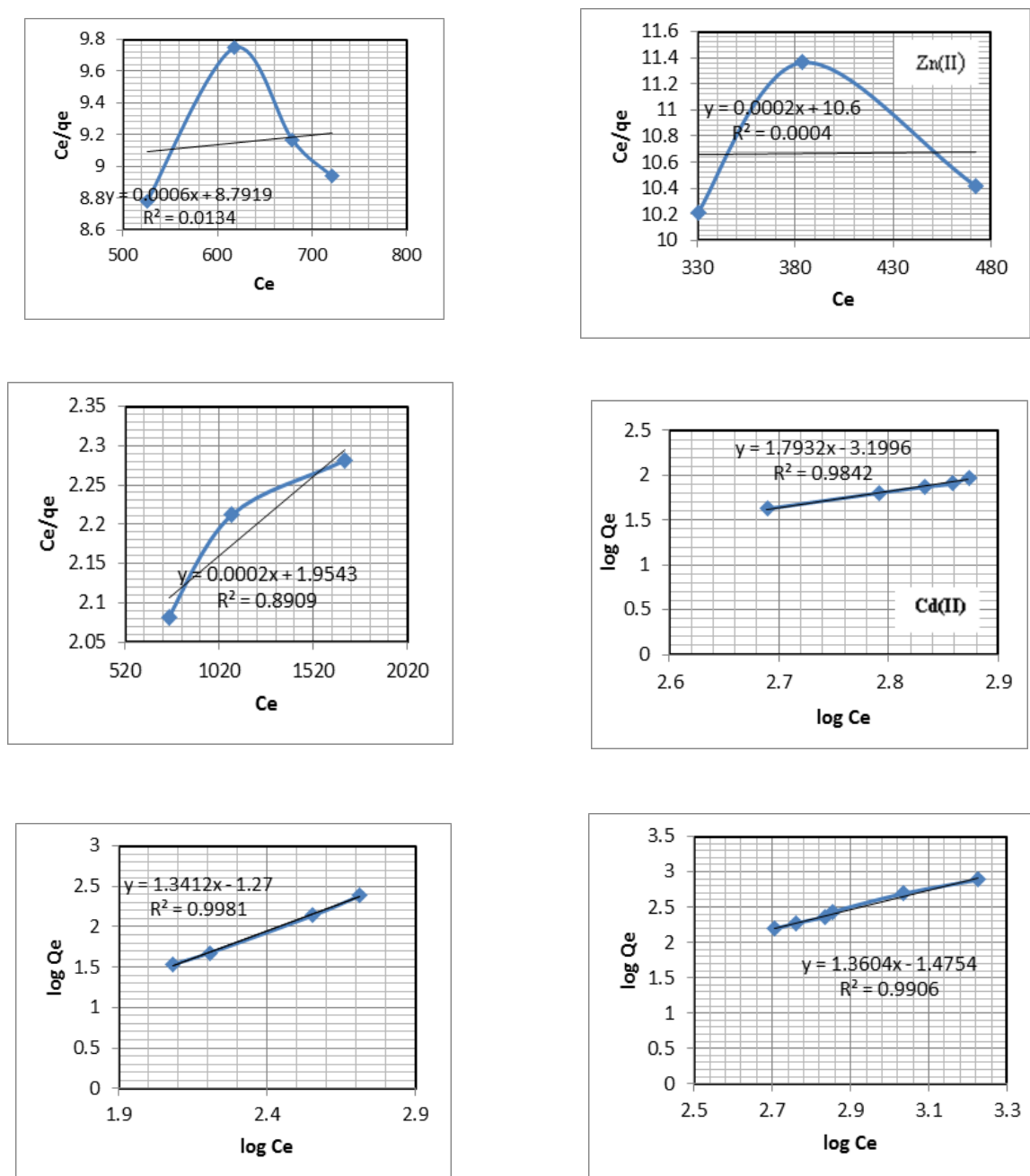


Fig. 9. Langmuir (a) (b) (c) and Freundlich (d) (e) (f) isotherm models plots for adsorption of Cd(II), Zn(II), and Pb(II) by AAc/CMC-TiO<sub>2</sub> hydrogel nanocomposite.

## References

- Hoffman, A.S., Hydrogels for biomedical applications. *Advanced Drug Delivery Reviews*, **64**,18-23(2012).
- Pensalfini, M., et al., Factors affecting the mechanical behavior of collagen hydrogels for skin tissue engineering. *Journal of the Mechanical Behavior of Biomedical Materials*, **69**,85-97(2017).
- Rakhshaei, R. and H. Namazi, A potential bioactive wound dressing based on carboxymethyl cellulose/ ZnO impregnated MCM-41 nanocomposite hydrogel. *Materials Science and Engineering: C*, **73**, 456-464(2017).
- Jonášová, E.P. and B.T. Stokke, Bioresponsive DNA-co-polymer hydrogels for fabrication of sensors. *Current Opinion in Colloid & Interface Science*, **26**, 1-8(2016).
- Treenate, P. and P. Monvisade, In vitro drug release profiles of pH-sensitive hydroxyethylacryl chitosan/sodium alginate hydrogels using paracetamol as a soluble model drug. *International Journal of Biological Macromolecules*, **99**,71-78(2017).
- Guilherme, M.R., et al., Superabsorbent hydrogels based on polysaccharides for application in agriculture as soil conditioner and nutrient carrier: A review. *European Polymer Journal*, **72**,365-385(2015).
- Khan, M. and I.M. Lo, Removal of ionizable aromatic pollutants from contaminated water using nano  $\gamma$ -Fe<sub>2</sub>O<sub>3</sub> based magnetic cationic hydrogel: Sorptive performance, magnetic separation and reusability. *Journal of Hazardous Materials*, **322**,195-204(2017).
- El-Mohdy, H.A., et al., Metal sorption behavior of poly (N-vinyl-2-pyrrolidone)/(acrylic acid-co-styrene) hydrogels synthesized by gamma radiation. *Journal of Environmental Chemical Engineering*, **1**(3),328-338(2013).
- Barbucci, R., A. Magnani, and M. Consumi, Swelling behavior of carboxymethylcellulose hydrogels in relation to cross-linking, pH, and charge density. *Macromolecules*, **33**(20),7475-7480(2000).
- Yetimoğlu, E.K., et al., N-vinylpyrrolidone/acrylic acid/2-acrylamido-2-methylpropane sulfonic acid based hydrogels: synthesis, characterization and their application in the removal of heavy metals. *Reactive and Functional Polymers*, **67**(5), 451-460(2007).
- Sakthivel, M., D. Franklin, and S. Guhanathan, pH-sensitive Itaconic acid based polymeric hydrogels for dye removal applications. *Ecotoxicology and Environmental Safety*, **134**, 427-432(2016).
- Wang, Y., et al., Removal of Methyl Violet from aqueous solutions using poly (acrylic acid-co-acrylamide)/attapulgit composite. *J. Environ. Sci*, **22**(1),7-14(2010).
- Pakdel, P.M. and S.J. Peighambaroust, A review on acrylic based hydrogels and their applications in wastewater treatment. *Journal of Environmental Management*, **217**,123-143(2018).
- Mahmoud, M.E., A.E. Abdou, and G.M. Nabil, Facile microwave-assisted fabrication of nano-zirconium silicate-functionalized-3-aminopropyltrimethoxysilane as a novel adsorbent for superior removal of divalent ions. *Journal of Industrial and Engineering Chemistry*, **32**,365-372(2015).
- Kadirvelu, K., K. Thamaraiselvi, and C. Namasivayam, Removal of heavy metals from industrial wastewaters by adsorption onto activated carbon prepared from an agricultural solid waste. *Bioresource Technology*, **76**(1),63-65(2001).
- Tao, Y., et al., Removal of Pb (II) from aqueous solution on chitosan/TiO<sub>2</sub> hybrid film. *Journal of Hazardous Materials*, **161**(2-3),718-722(2009).
- Mahmoud, M.E., et al., Solid-solid crosslinking of carboxymethyl cellulose nanolayer on titanium oxide nanoparticles as a novel biocomposite for efficient removal of toxic heavy metals from water. *Int J Biol Macromol*, **105**(Pt 1),1269-1278(2017).
- Morán Quiroz, J.L., et al., Polymeric hydrogels obtained using a redox initiator: Application in Cu (II) ions removal from aqueous solutions. *Journal of Applied Polymer Science*, **131**(4), (2014).
- Anirudhan, T. and S. Sreekumari, Synthesis and characterization of a functionalized graft copolymer of densified cellulose for the extraction of uranium (VI) from aqueous solutions. *Colloids and Surfaces A: Physicochemical and Engineering Aspects*, **361**(1-3),180-186 (2010).
- Zheng, Y., D. Huang, and A. Wang, Chitosan-g-poly (acrylic acid) hydrogel with crosslinked polymeric networks for Ni<sup>2+</sup> recovery. *Analytica Chimica Acta*, **687**(2),193-200(2011).

21. Yang, S., et al., Hydrogel beads based on carboxymethyl cellulose for removal heavy metal ions. *Journal of Applied Polymer Science*, **119**(2), 1204-1210(2011).
22. El-Hag Ali, A., Removal of heavy metals from model wastewater by using carboxymethyl cellulose/2-acrylamido-2-methyl propane sulfonic acid hydrogels. *Journal of Applied Polymer Science*, **123**(2),763-769(2012).
23. Kurdtabar, M., et al., Biocompatible Magnetic Hydrogel Nanocomposite Based on Carboxymethylcellulose: Synthesis, Cell Culture Property and Drug Delivery. *Polymer Science, Series B*, **60**(2), 231-242(2018).
24. Bozaci, E., Application of carboxymethylcellulose hydrogel based silver nanocomposites on cotton fabrics for antibacterial property. *Carbohydrate Polymers*, **134**,128-135(2015).
25. Pejman Hadi, J.B., Gordon McKay, Synergistic effect in the simultaneous removal of binary cobalt–nickel heavy metals from effluents by a novel e-waste-derived material. *Chemical Engineering Journal*, **228**,140-146(2013).
26. Razzaz, A., et al., Chitosan nanofibers functionalized by TiO<sub>2</sub> nanoparticles for the removal of heavy metal ions. *Journal of the Taiwan Institute of Chemical Engineers*, **58**,333-343(2016).
27. Mahmoud, M.E., et al., High performance SiO<sub>2</sub>-nanoparticles-immobilized-Penicillium funiculosum for bioaccumulation and solid phase extraction of lead. *Bioresour Technol*, **106**,125-32(2012).
28. Mahmoud, M.E., et al., Adsorptive Removal of Zn (II), Co (II) and Their Radioactive Isotopes <sup>65</sup> Zn, <sup>60</sup> Co on The surface of sodium nano bentonite coated with oleyl-amine. *J Radiat Nucl Appl*, **2**, 87-93(2017).
29. Mahmoud, M.E., A.A. Soayed, and O.F. Hafez, Selective Solid Phase Extraction and Pre-Concentration of Heavy Metals from Seawater by Physically and Chemically Immobilized 4-Amino-3-Hydroxy-2-(2-Chlorobenzene)-Azo-1-Naphthalene Sulfonic Acid Silica Gel. *Microchimica Acta*, **143**,65–70(2003).
30. Mahmoud, M.E., M.T. Abou Kana, and A.A. Hendy, Synthesis and implementation of nano-chitosan and its acetophenone derivative for enhanced removal of metals. *Int J Biol Macromol*, **81**, 672-80(2015).
31. Quintelas, C., et al., Competitive biosorption of ortho-cresol, phenol, chlorophenol and chromium (VI) from aqueous solution by a bacterial biofilm supported on granular activated carbon. *Process Biochemistry*, **41**(9), 2087-2091(2006).
32. Sadeek, S.A., et al., Metal adsorption by agricultural biosorbents: Adsorption isotherm, kinetic and biosorbents chemical structures. *International Journal of Biological Macromolecules*, **81**, 400-409(2015).
33. Demirbas, A., Heavy metal adsorption onto agro-based waste materials: A review. *Journal of Hazardous Materials*, **157**(2-3), 220-229(2008).
34. Ho, Y.-S. and G. McKay, The kinetics of sorption of divalent metal ions onto sphagnum moss peat. *Water Research*, **34**(3), 735-742(2000).
35. Ho, Y. and C. Chiang, Sorption studies of acid dye by mixed sorbents. *Adsorption*, **7**(2), 139-147(2001).
36. Yuh-Shan, H., Citation review of Lagergren kinetic rate equation on adsorption reactions. *Scientometrics*, **59**(1), 171-177(2004).
37. Alley, E.R., *Water Quality Control Handbook*. Vol. 2, McGraw-Hill New York(2007).
38. Mahmoodi, N.M., et al., Dye adsorption and desorption properties of Mentha pulegium in single and binary systems. *Journal of Applied Polymer Science*, **122**(3),1489-1499(2011).
39. Febrianto, J., et al., Equilibrium and kinetic studies in adsorption of heavy metals using biosorbent: a summary of recent studies. *Journal of Hazardous Materials*, **162**(2-3), 616-645(2009).

## استخدام نانومتراكب هيدروجيل الكربوكسي مثيل سيليلوز/حمض اكرليك/ ثاني أكسيد التيتانيوم في تطبيق معالجة المياه لأزالة ايونات Cd(II), Zn(II) , Pb(II)

أحمد عبد العليم هندي<sup>1</sup>، إيهاب السيد الخزيمي<sup>2</sup>، غادة عادل محمود<sup>2</sup>، إبتسام أحمد سعد<sup>3</sup>، شريف حسني سرور<sup>1</sup>  
الشركة القابضة للمياه والصرف الصحي - القاهرة - مصر.  
<sup>2</sup>المركز القومي لبحوث وتكنولوجيا الإشعاع - هيئة الطاقة الذرية - مدينة نصر - القاهرة - مصر - ص.ب. 22  
<sup>3</sup>كلية العلوم - جامعة عين شمس - القاهرة - مصر - ص.ب. 86

في هذه الدراسة تم تصنيع حمض الاكرليك/كاربوكسي ميثيل سلولوز/ثاني أكسيد التيتانيوم (AAc/CMC-TiO<sub>2</sub>) هيدروجيل نانوكومبوسيت عن طريق البلمرة المختلطة بواسطة الشوارد الحرة عبرالتشيع الجامي. وتم توصيفه باستخدام مطياف الأشعة تحت الحمراء FT-IR وخصائص التورم. وجد ان نسبة التورم تزداد مع زيادة الوقت حتى تصل إلى قيمة ثابتة بعد 6 ساعات. تم استخدام مركب النانو المحضر كمادة ممتزة لمعالجة ايونات الكاديوم والخاصين والرصاص من المحاليل المائية بواسطة تقنية الامتزاز الاستاتيكي. وقد وجد أن الرقم الهيدروجيني الأمثل للامتزاز هو 5 ويتم تنفيذ عملية الامتزاز في وقت تشغيل سريع، 30-40 دقيقة، لجميع أيونات المعادن التي تم فحصها. وقد وجد أيضًا أن قدرة امتزاز أيونات المعادن تتناقص مع زيادة جرعة المادة الممتزة من 5 إلى 150 مجم. تم الحصول على زيادة تدريجية في قدرة امتصاص أيونات المعادن بزيادة تركيز أيون المعدن الأولي من 0.01 إلى 0.05 مولر وتم تشبع المواقع النشطة الماصة عند تركيز أيونات المعادن الأولية عند 0.1 مولر. لم يحدث أي تداخل كبير على إزالة الرصاص في وجود كلوريد الصوديوم واسيتات الصوديوم وكلوريد البوتاسيوم ونترات البوتاسيوم وكلوريد الامونيوم بينما حدث انخفاض طفيف في إزالة الكاديوم والخاصين. وجد ان نموذج الحركة من الدرجة الثانية الزائفة ونموذج امتزاز Freundlich يصف جيدا الحركة والأيزوثرم لعملية الامتزاز للأيونات التي تم فحصها.